

Comparison of Vector and Scalar Modes in a Lightguide with a Hyperbolic Secant Index Distribution

By G. E. PETERSON, A. CARNEVALE, and U. C. PAEK

(Manuscript received May 30, 1980)

To develop a sound base on which to design efficient lightguides, it is necessary to understand the physics of the propagating modes of this transmission medium. In this paper, we examine the properties of the scalar modes in an infinite lens-like medium and the vector modes in a self-focusing fiber with an infinite homogeneous cladding for a hyperbolic secant index distribution. We find that only the meridional rays are equalized and that this only occurs when there is no material dispersion.

I. INTRODUCTION

As is well known, the index distribution

$$N(x) = N_0 \operatorname{sech} gx \quad (1)$$

has an ideal focusing property for a two-dimensional medium.¹⁻⁴ The group velocities of the various modes are equalized, and if the medium is dispersion-free the group velocities are independent of frequency as well. It is believed that, for a cylindrical lightguide where the index is a function of the radius, such an optimum distribution does not exist.¹ In particular, a distribution of the sort

$$N(r) = N_0 \operatorname{sech} gr, \quad (2)$$

where r is the radius, will not be expected to have ideal focusing properties. In fact, in the presence of material dispersion, the distribution described by eq. (2) is expected to be similar to a parabolic distribution.

The properties of the distribution described by eq. (2) can most easily be inferred from an analysis of the scalar modes in an infinite lens-like medium.^{1,5-9} The purpose of this work is to review these

properties and then compare them with an exact numerical analysis of the vector modes in a self-focusing fiber with an infinite homogeneous cladding.

II. RELATIONSHIP BETWEEN SCALAR AND VECTOR MODES

The vector modes¹⁰⁻¹² in a lightguide are normally specified as $HE_{m,q}$, $EH_{m,q}$, $TE_{o,q}$, and $TM_{o,q}$, where m is the polar index and q the radial index. Far from cutoff, relationships between the radial field functions for the vector modes ϕ and the scalar modes ψ can be established.¹³ They are

$HE_{m,q}$ modes

$$\phi_{m,q} \approx \psi_{m-1,q-1} \quad (3)$$

$EH_{m,q}$ modes

$$\phi_{m,q} \approx \psi_{m+1,q-1} \quad (4)$$

$TE_{o,q}$ modes

$$\phi_{o,q} \approx \psi_{1,q-1} \quad (5)$$

$TM_{o,q}$ modes

$$\phi_{o,q} \approx \psi_{1,q-1}. \quad (6)$$

Likewise, relationships can also be established between the effective indices N_e . They are

	<i>Vector Modes</i>	<i>Scalar Modes</i>	
HE	$N_e(m, q)$	$N_e(m-1, q-1)$	(7)
EH	$N_e(m, q)$	$N_e(m+1, q-1)$	(8)
TE	$N_e(o, q)$	$N_e(1, q-1)$	(9)
TM	$N_e(o, q)$	$N_e(1, q-1).$	(10)

III. SOME PROPERTIES OF SCALAR MODES

Consider now the following dispersion-free index distribution for an infinite lens-like medium

$$N^2(r) = N_o^2[1 - (r/L)^2 + \delta(r/L)^4], \quad (11)$$

where $2\pi L$ represents the paraxial focal length of the medium. When $\delta = 2/3$, this function approximates eq. (2) closely and, when $\delta = 0$, it approximates a parabolic index distribution. For the scalar radial field function $\psi_{\alpha,\beta}$, one finds from a first-order perturbation calculation that

the effective indices can be written as¹

$$N_e^2 = N_o^2 - \frac{N_o A}{2\pi/\lambda} + \frac{B}{(2\pi/\lambda)^2}, \quad (12)$$

where

$$A = 2(2\beta + \alpha + 1)/L, \quad (13)$$

$$B = \delta[6\beta^2 + 6\beta(\alpha + 1) + (\alpha + 1)(\alpha + 2)]/L^2, \quad (14)$$

and λ is the wavelength. If we substitute $\delta = \frac{2}{3}$ and let $\alpha = 1$, we get the result

$$N_e = N_o - \frac{2[\beta + 1]}{(2\pi/\lambda)L}. \quad (15)$$

This tells us that the difference in effective index between adjacent scalar modes with $\alpha = 1$ is a constant. By means of (9) and (10), we predict the identical result for the tightly bound TE and TM vector modes.

Also, from first-order perturbation theory, it can be shown that¹

$$N_g = \frac{N_o[(2\pi/\lambda) \cdot N_o - A/2]}{[(2\pi/\lambda)^2 \cdot N_o^2 - (2\pi/\lambda)N_o A + B]^{1/2}}, \quad (16)$$

where N_g is the group index. Again, if we substitute $\delta = \frac{2}{3}$ and let $\alpha = 1$, we obtain another interesting result, namely,

$$N_g = N_o. \quad (17)$$

This tells us that all scalar modes with $\alpha = 1$ have the same group index and this index is N_o . Equations (5) and (6) predict the same result for the tightly bound TE and TM vector modes. One would *not* expect this to be the case for general EH or HE vector modes, however. This latter point will be examined by the numerical methods to be described shortly. As pointed out by Kawakami,¹ scalar waves $\psi_{\alpha,\beta}$ when $\alpha \approx 0$ are meridional rays and when $\beta \approx 0$ are helical rays. From eqs. (3) to (10) and (17), we conclude that the tightly bound TE and TM vector modes are meridional rays. Similarly, tightly bound EH and HE vector modes with high polar indices m and low radial indices q would be helical rays.

Let us now apply the previous results for scalar waves to a lightguide. We consider a guide with a core center index of 1.47428 and at a wavelength of 0.82 microns. The parameters N_o and L in eq. (11) are chosen so that, at an r of zero, we obtain the core center index and at an r of 25 microns we have an index of 1.45330. This allows us to make a good comparison with the vector modes in a self-focusing fiber that is considered in the next section. We again assume the medium is dispersion-free.

Figure 1 shows the group index N_g of helical and meridional rays as

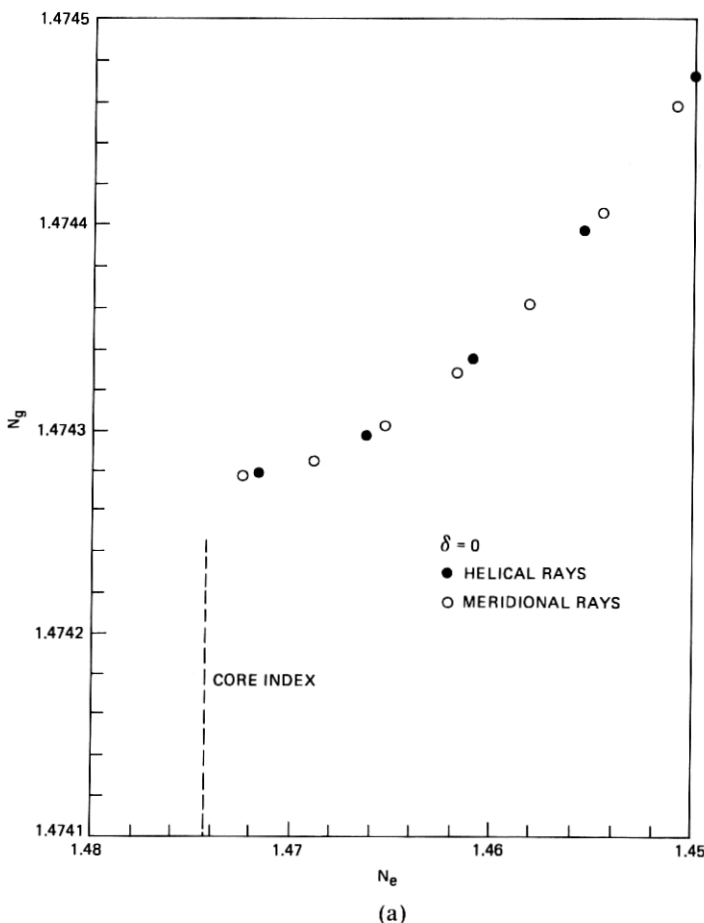


Fig. 1—The group index N_g as a function of effective index N_e as calculated from eqs. (12) and (16) for meridional and helical rays. The meridional rays are plotted as \circ while the helical rays are plotted as \bullet . In (a), $\delta = 0$ and the profile is parabolic. In (b), $\delta = \frac{1}{3}$ and there is a separation between helical and meridional rays. In (c), $\delta = \frac{2}{3}$ and the profile is a hyperbolic secant. We note that the group index of the meridional rays is constant. In (d), $\delta = 1$ and we note that the helical rays have the same group index.

a function of effective index for four values of δ , namely, 0, $\frac{1}{3}$, $\frac{2}{3}$, and 1. When $\delta = 0$, we have a parabolic index distribution and we see that the helical and meridional rays lie on coincident curves. In fact, all other rays are coincident as well. We note substantial dispersion of the group index with effective index.

When $\delta = \frac{1}{3}$, the curves for the helical and meridional rays begin to separate. The other rays distribute themselves between these two curves. One still notes substantial dispersion of the group index with effective index. When $\delta = \frac{2}{3}$, we very closely approximate a hyperbolic

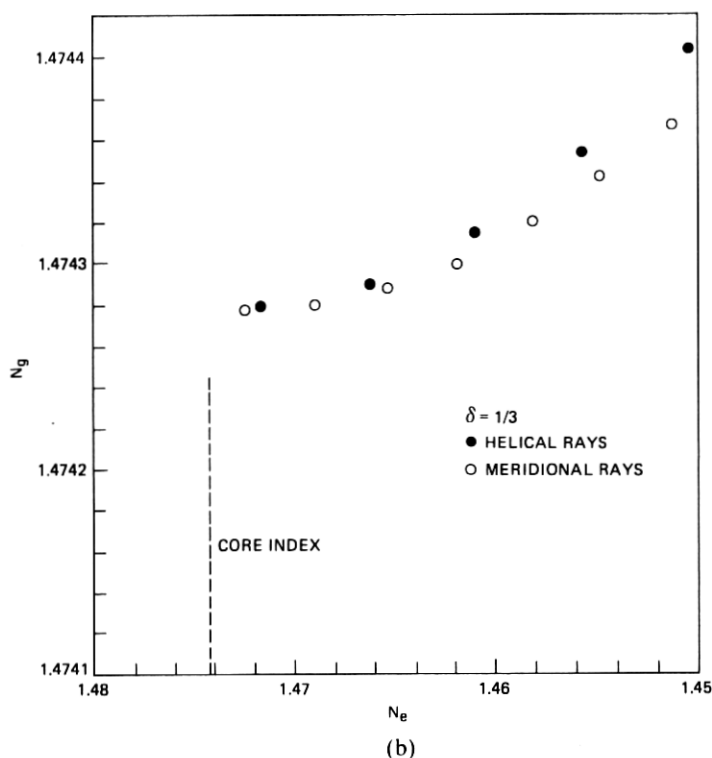


Fig. 1—continued.

secant index profile. The meridional rays now all have the same group index or, in other words, are equalized. The helical rays and all other rays show varying degrees of dispersion.

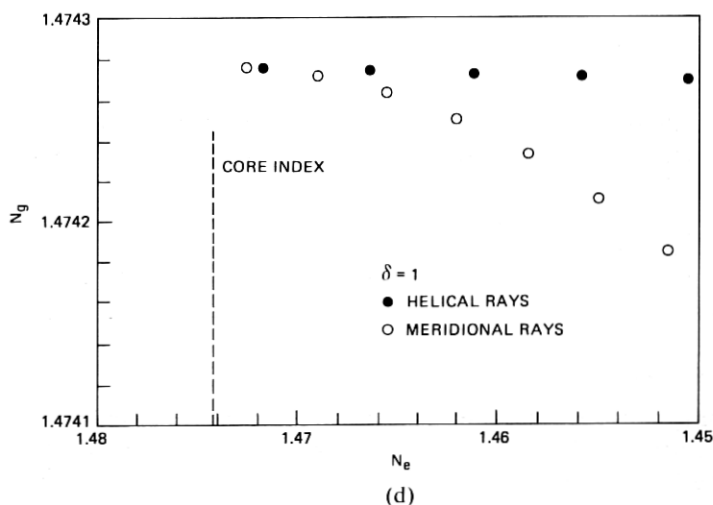
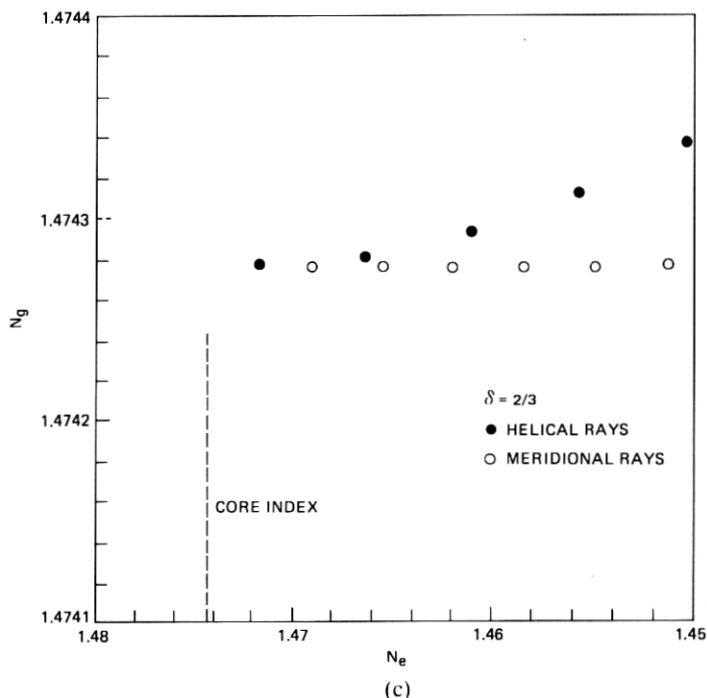
When $\delta = 1$, the helical rays are well equalized but now the meridional rays and all other rays show dispersion. Quite obviously, there is no distribution in index of the form described by eq. (11) that would equalize the scalar modes in an infinite lens-like medium.

III. VECTOR MODES

Using numerical methods, we can obtain rigorous solutions to the vector form of Maxwell's equations for any index distribution.¹⁴⁻¹⁶ The method we employ is similar to that of Vigants and Schlesinger¹⁴ and uses an optimized fourth-order Runge-Kutta procedure¹⁷ with double precision arithmetic. The group indices can be calculated from the effective indices by the following formula:

$$N_g = N_e - \lambda dN_e/d\lambda. \quad (18)$$

We consider the exact hyperbolic secant profile, eq. (2), rather than



chosen so that, when $r = 25$ microns, the function gives the correct value for the cladding index and N_o is the index at the core center. We also consider an exact parabolic-index profile rather than that given approximately by eq. (11) with $\delta = 0$. This profile is tailored to match the core-center index and the cladding index.

From the discussion in the previous section and eq. (15), we would expect the difference in effective index to be the same between adjacent TE or TM vector modes for the hyperbolic secant profile. In Fig. 2, we plot this difference for the sequence of TM modes. We see that, for all except the last two modes, this spacing is indeed constant. The same result is found for the TE modes. These latter two modes cannot be considered tightly bound because of the finite size of the core of the lightguide. Thus, (15) would not apply to them. This change in character of these modes clearly demonstrates the strong influence of the core-cladding interface. The spacing between adjacent TE or TM vector modes for the parabolic index profile would not be expected to be the same. That this is the case is also shown in Fig. 2. The influence of the core-cladding interface is evident here as well.

From eq. (17) and earlier discussion, we would expect that all the TE and TM vector modes for the hyperbolic secant profile would have the same group index. In Fig. 3, we plot the group index for the TE modes as a function of effective index. For all practical purposes, the group indices are the same except again for the last few modes. The result is

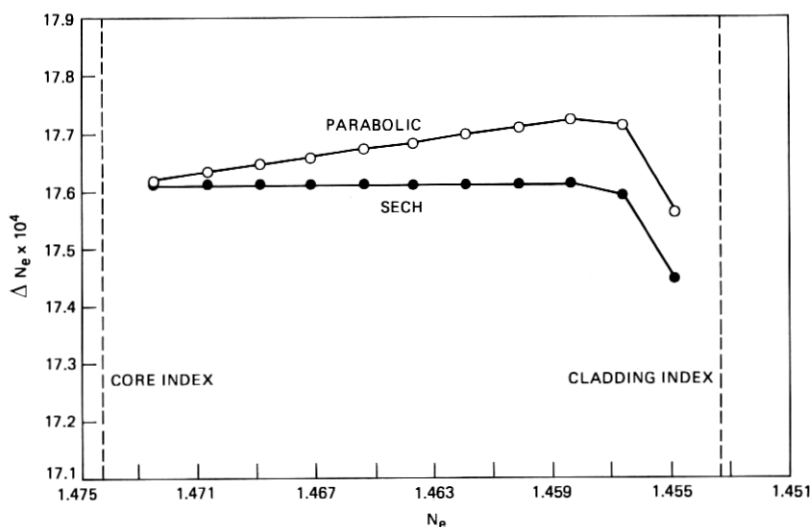


Fig. 2—Plot of ΔN_e versus N_e for the TE or TM vector modes for a fiber with a hyperbolic secant and parabolic index profile. TE and TM vector modes correspond to meridional rays. This shows that there is no difference between the effective indices of adjacent, tightly bound modes.

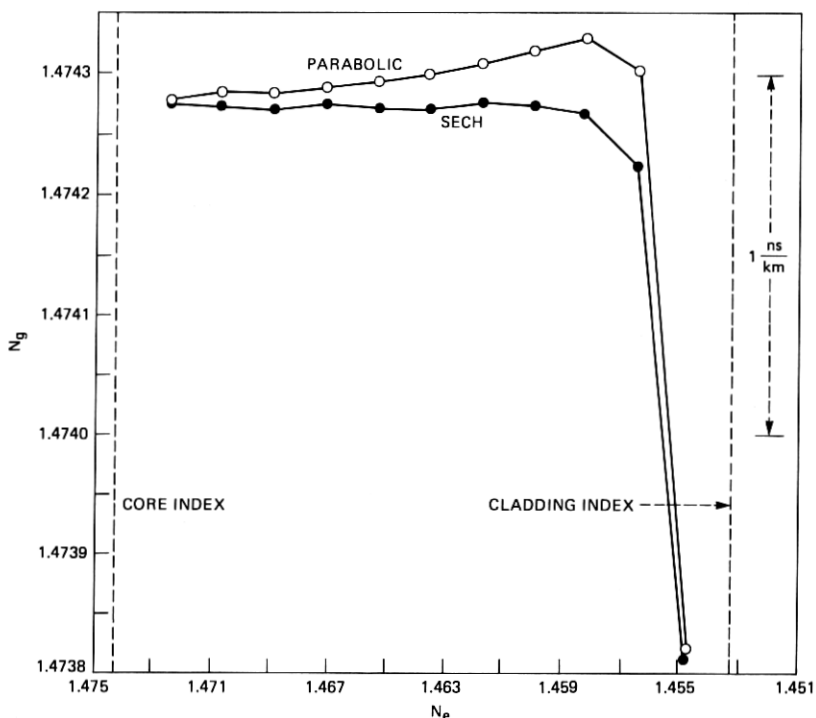


Fig. 3—Plot of N_g versus N_e for the TE or TM vector modes for a fiber with a hyperbolic secant and a parabolic index profile. For the hyperbolic secant profile, we see that the meridional rays have the same group index except for those that are influenced by the cladding.

identical for the TM mode. The average value of group index, if we do not include the last modes, is 1.47427. From eq. (17), we would expect this to be 1.47428. The agreement is excellent. It should be remembered that the TE or TM modes are the meridional rays. Thus the meridional rays are seen to be equalized in a lightguide with a hyperbolic secant profile, except, of course, the last few, which are being influenced by the cladding. Figure 3 also shows the result for the meridional rays when the profile is parabolic. Clearly, these rays do not all have the same group index.

From (16), we expect only the TE and TM modes to be equalized in a fiber with a hyperbolic secant index distribution. In other words, skew rays would have different group indices from meridional rays. That this is indeed the case can be seen in Fig. 4. The dots correspond to the group indices of the vector modes with polar indices 4, 8, 12, 14, 16, 18, and 20. The solid lines are calculated from eq. (16). The upper one is for helical scalar modes, and the lower one for meridional scalar modes. It is clear that the vector modes for non-meridional rays are

not equalized, and the spread is very similar to that predicted by the scalar theory. The strong influence of the cladding on the vector modes is again made very clear.

When material dispersion becomes dominant, such as would be the case at 0.82 micron for a germania-doped silica lightguide, we would expect great similarity between the group indices of a fiber with a parabolic index and a fiber with a hyperbolic secant index distribution. Figure 5 shows the group indices for the TE vector modes for both these profiles with material dispersion effects included exactly in the calculation. The material dispersion parameters are taken from the work of Fleming^{18,19} of 13-mole percent doped silica and pure silica. The very strong effect of the materials dispersion is evident. In addition, the influence of the cladding on the last two modes is again noted.

IV. CONCLUSIONS

The scalar modes in an infinite lens-like medium can indeed predict some of the properties of the vector modes in a self-focusing fiber with

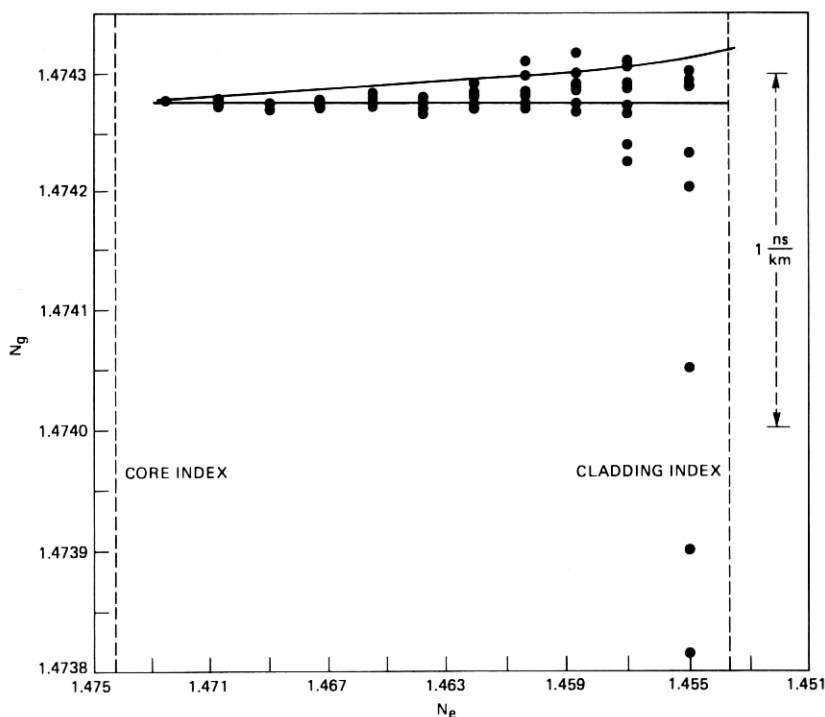


Fig. 4—The dots correspond to the group indices of the vector modes with polar indices 4, 8, 12, 14, 16, 18, and 20. The solid lines are scalar modes calculated from eq. (16). The upper line is for helical rays and the lower one for meridional rays.

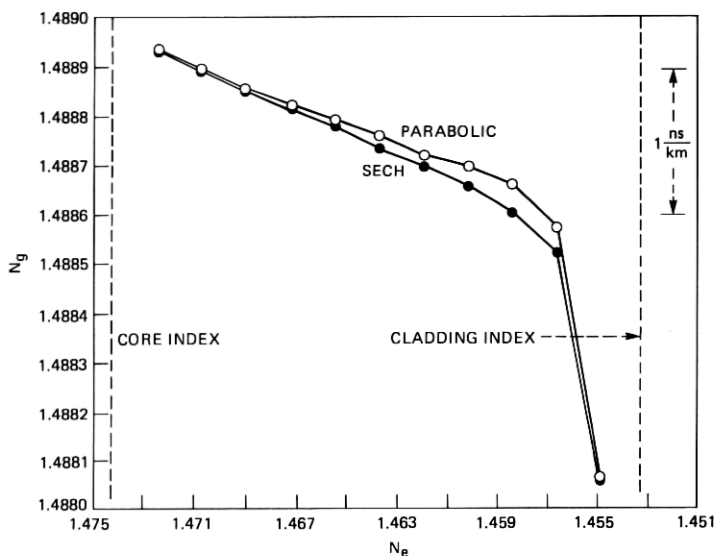


Fig. 5—A comparison of the group indices for a hyperbolic secant profile and a parabolic profile in the presence of material dispersion. The wavelength is 0.82 micron, and the core center is silica-doped with 13-mole percent germania.

an infinite homogeneous cladding. Perhaps the most striking difference are those modes that are influenced by the cladding. A more subtle difference is that the vector modes tend to be more dispersive, as is evidenced by Fig. 4. The belief that, for a cylindrical lightguide, a distribution of the sort given by eq. (2) (i.e., hyperbolic secant distribution) *only* equalizes meridional rays is well substantiated by the rigorous vector mode analysis. Finally, we see that in the presence of strong material dispersion there is no outstanding advantage of the hyperbolic secant-index distribution over the parabolic-index distribution.

REFERENCES

1. S. Kawakami and J. Nishizawa, "An Optical Waveguide With the Optimum Distribution of Refractive Index With Reference to Waveform Distortion," *IEEE Trans., MTT-16* (October 1968), pp. 814-818.
2. E. T. Kornhauser and A. D. Yaghjian, "Modal Solution of a Point Source in a Strongly Focusing Medium," *Radio Science*, 2 (March 1967), pp. 299-310.
3. E. G. Rawson, D. R. Herriott, and J. McKenna, "Analysis of Refractive Index Distributions in Cylindrical, Graded Index Glass Rods (GRIN Rods) Used as Image Relays," *Appl. Opt.*, 9 (March 1970), pp. 753-759.
4. S. Cornbleet, "Ray Paths in a Uniform Axially Symmetric Medium," *IEEE J. Microwave Optics and Acoustics*, 2 (November 1978), pp. 194-200.
5. D. Marcuse, "The Impulse Response of an Optical Fiber With Parabolic Index Profile," *B.S.T.J.*, 52 (September 1973), pp. 1169-1174.
6. D. Gloge and E. A. J. Marcatili, "Multimode Theory of Graded-Core Fibers," *B.S.T.J.*, 52 (November 1973), pp. 1563-1578.
7. E. A. J. Marcatili, "Modes in a Sequence of Thick Astigmatic Lens-Like Focusers," *B.S.T.J.*, 43 (November 1964), pp. 2887-2904.

8. D. Marcuse, *Light Transmission Optics*, New York: Van Nostrand, 1972, Chap. 7.
9. M. Matsuhara, "Analysis of TEM Modes in Dielectric Waveguides by a Variational Method," *J. Opt. Soc. Am.*, **63** (December 1973), pp. 1514-1517.
10. G. L. Yip and Y. H. Ahmew, "Propagation Characteristics of a Radially Inhomogeneous Optical Fiber," *Electron. Lett.*, **10** (February 1974), pp. 37-38.
11. J. G. Dil and H. Blok, "Propagation in Graded Index Optical Fibers," *Opto-Electronics*, **5** (May 1973), pp. 415-420.
12. S. Ishikawa, K. Furaya, Y. Suematsu, "Vector Wave Analysis of Broadband Multimode Optical Fibers With Optimum Refractive Index Distribution," *J. Opt. Soc. Am.*, **68** (May 1978), pp. 577-583.
13. G. L. Yip and S. Nemoto, "The Relations Between Scalar Modes in a Lenslike Medium and Vector Modes in a Self-Focusing Optical Fiber," *IEEE Trans., MTT-23* (February 1975), pp. 260-263.
14. A. Vigants and S. P. Schlesinger, "Surface Waves on Radially Inhomogeneous Cylinders," *IEEE Trans., MTT-10* (September 1962), pp. 375-382.
15. G. E. Peterson, A. Carnevale, U. C. Paek, and D. W. Berreman, "An Exact Numerical Solution to Maxwell's Equations for Lightguides," *B.S.T.J.*, **59**, No. 7 (September 1980), pp. 1175-1196.
16. M. O. Vassel, "Calculation of Propagating Modes in a Graded Index Optical Fiber," *Opto-Electronics*, **6** (July 1974), pp. 271-286.
17. A. Ralston, "Runge-Kutta Methods With Minimum Error Bounds," *Mathematics of Computation*, **16** (October 1962), pp. 431-437.
18. J. W. Fleming, "Material and Mode Dispersion in $\text{GeO}_2 \cdot \text{B}_2\text{O}_3 \cdot \text{SiO}_2$ Glasses," *J. Am. Ceram. Soc.*, **59** (November-December, 1976), pp. 503-507.
19. J. W. Fleming, "Material Dispersion in Lightguide Glasses," *Electron. Lett.*, **14** (May 1978), pp. 326-328.

